Phase matching using Bragg reflection waveguides for monolithic nonlinear optics applications

A. S. Helmy

Edward S. Rodgers Department of Electrical and Computer Engineering, University of Toronto, Toronto, ON M5S 3G4, Canada
a.helmy@utoronto.ca

http://photonics.light.utoronto.ca/helmy/

Abstract: A novel design to achieve phase matching between modes of a vertical distributed Bragg reflector waveguide and those of a conventional total internal reflection waveguide is reported for the first time. The device design and structure lend themselves to monolithic integration with active devices using well developed photonic fabrication technologies. Due to the lack of any modulation of the optical properties in the direction of propagation, the device promises very low insertion loss. This property together with the large overlap integral between the interacting fields dramatically enhances the conversion efficiency. The phase matching bandwidth, tunability and dimensions of these structures make them excellent contenders to harness optical nonlinearities in compact, low insertion loss monolithically integrable devices.

OCIS codes: (130.3120) Integrated optics devices; (230.7370) Waveguides; (230.1480) Bragg reflectors (190.2620) Nonlinear optics Frequency conversion
(190.4390) Nonlinear optics : Nonlinear optics, integrated optics.

References and links

1. C. B. Ebert, L. A. Eyres, M. M. Fejer, J. H. Harris, "GaAs/Ge/GaAs sublattice reversal epitaxy and its application to nonlinear optical devices," J. Cryst. Growth **227**, 183-192 (1999).
2. J. B. Khurgin, E. Rosencher, Y. J. Ding, "Analysis of all-semiconductor intracavity optical parametric oscillators," J. Opt. Soc. Am. B **15**, 1726-1734 (1998).
3. A. Fiore, S. Janz, L. Delobel, P. van der Meer, P. Bravetti, V. Berger, and E. Rosencher, "Second-harmonic generation at λ= 1.6 μm in AlGaAs/Al_2O_3 waveguides using birefringence phase matching," Appl. Phys. Lett. **72**, 2942-2945 (1998).
4. A. S. Helmy, D. C. Hutchings, T. C. Kleckner, J. H. Marsh, A. C. Bryce, J. M. Arnold, C. R. Stanley, and J. S. Aitchison, C. T. A. Brown, K. Moutzouris and M. Ebrahimzadeh, "Quasi phase matching in GaAs-AlAs superlattice waveguides via bandgap tuning using quantum well intermixing," Opt. Lett. **25**, 1370-1373 (2000).
5. R. Haidar, N. Forget, E. Rosencher, "Optical parametric oscillation in micro-cavities based on isotropic semiconductors: a theoretical study," IEEE J. Quantum Electron. **39**, 569-576 (2003).
6. D. Faccio, F. Bragheri, M. Cherchi, "Optical Bloch-mode-induced quasi phase matching of quadratic interactions in one-dimensional photonic crystals," J. Opt. Soc. Am. B **21**, 296-301 (2004).
7. K. L. Vodopyanov, O. Levi, P.S. Kuo, T.J. Pinguet, J.S. Harris, M.M. Fejer, B. Gerard, L. Becouarn, E. Lallier "Optical parametric oscillation in quasi-phase-matched GaAs," Opt. Lett. **29**, 1912-1914, (2004).
8. A. S. Helmy, Brian R. West "Phase Matching using Bragg Reflector Waveguides," IEEE LEOS Annual Meeting, Sydney, (2005).
9. P. Yeh, A. Yariv, " Bragg reflection waveguides," Opt. Commun. **19**, 427-430 (1976).
10. P. Yeh, A. Yariv, C Hong "Electromagnetic propagation in periodic stratified media: I. General Theory," J. Appl. Phys., **67**, 423-438 (1977).
11. S. R. A. Dods, "Bragg reflection waveguides," J. Opt. Soc. Am. A, **6**, 1465-1475 (1989).
12. E. Simova, I. Golub, "Polarization splitter/combiner in high index contrast reflector waveguides," Opt. Express **11**, 3425-3430 (2003).

#10071 - $15.00 USD Received 21 December 2005; revised 30 January 2006; accepted 31 January 2006

13. A. Mizrahi, L. Schächter, "Bragg reflection waveguides with a matching layer," Opt. Express **12**, 3156-3170 (2004).
14. C. Wätcher, F. Lederer, L. Leine, U. Trutschel, M. Mann, " Nonlinear Bragg reflection waveguide," J. Appl. Phys. **71**, 3688-3692 (1992).
15. P. M. Lambkin, K. A. Shore, "Nonlinear semiconductor Bragg reflection waveguide structures," IEEE J. Quantum Eletron. **27**, 824-828 (1991).
16. T. C. Kleckner, A. S. Helmy, K. Zeaiter, D. C. Hutchings, J. S. Aitchison, "Dispersion and Modulation of the Linear Optical Properties of GaAs/AlAs Superlattices Waveguides using Quantum Well Intermixing," IEEE J. Quantum Eletron. (Accepted).
17. P. Yeh, *Optical Waves in layered media*, (Wiley, 1988).
18. J. Chilwell, I. Hodgkinson, "Thin-film field-transfer matrix theory of planar multilayer waveguides and reflection from prism-loaded waveguides," J. Opt. Soc. Am. A **1**, 742-753 (1984)
19. J. Khurgin, "Improvement of frequency-conversion efficiency in waveguides with rotationally twinned layers," Opt. Lett, **13**, 603-605 (1988).
20. S. Ducci, L. Lanco, V. Berger, A. De Rossi, V. Ortiz, M. Calligaro, "Continuous-wave second-harmonic generation in modal phase matched semiconductor waveguides," Appl. Phys. Lett. **84,** 2974-2976 (2004).
21. P. Dong, A. G. Kirk, "Nonlinear frequency conversion in waveguide directional couplers," Phys. Rev. Lett. **93,** 133901 (2004).
22. N. Yokouchi, A. J. Danner, K. D. Choquette, "Two-dimensional photonic crystal confined vertical-cavity surface-emitting lasers," IEEE J. Sel. Top. Quantum Electron., **9**, 1439-1447 (2003).

1. Introduction

Optical parametric oscillators (OPOs) have become indispensable coherent sources for the mid infra red. Their operating wavelength span is limited by the transparency window of lithium niobate however, because periodically poled lithium niobate (PPLN) is the most commonly used nonlinear element in OPOs. Compound semiconductors such as GaAs, in contrast, exhibit higher nonlinear coefficients near the material resonances in comparison to PPLN, and have a large transparency window. In the case of GaAs the transparency window spans the spectral range 1-17 μm. GaAs also has high optical damage threshold and a mature fabrication technology for making waveguides in comparison to PPLN. Therefore, achieving parametric oscillation in semiconductors monolithically can vastly improve the efficiency of this class of coherent sources [1]. More importantly, the potential for monolithically integrating these nonlinear elements with active sources to form an OPO chip is an attractive option for numerous applications. A coherent source in this form factor is bound to redefine how coherent sources are used due to its versatility, ruggedness, and compactness [2]. It is clear, however, that achieving efficient, low loss and tunable phase matching in a semiconductor material is pivotal for the realization of the monolithic OPOs discussed.

Although semiconductors possess large nonlinearities, they also have large dispersion, particularly at wavelengths close to their bandgap. This makes the problems of phase matching challenging in such material systems. In order to phase match the two interacting waves, their wave vectors must obey the relation $k_{2\omega} = 2k_{\omega}$ which leads to the condition that requires the effective indices of both waves to be equal in order for perfect phase matching to occur, namely $n_{2\omega} = n_{\omega}$. The difficulty of achieving this in semiconductors is usually most severe while operating near the bandgap resonances where dispersion prevents such condition from naturally taking place. Various means have been devised to overcome this problem; form birefringence [3], quasi-phase matching [4], high Q resonant cavities [5] and photonic bandgap structures were all studied [6]. On one hand, these solutions produce a route to phase matching; however, they provide devices that are difficult to integrate with other active and passive photonic components. One of these approaches, which uses quasi-phase matching, lends itself to monolithic integration. However, so far it provides imperfect quasi-phase matching which makes the attainable effective nonlinearity too low to be of practical use [4]. Another very promising demonstration of quasi-phase matching in semiconductors relies on inverting the domain of the nonlinearity by growing the semiconductor with different orientations, and hence perfect quasi-phase matching has been reported [1]. Monolithic integration using this technique is yet to be demonstrated though, and is likely to prove

#10071 - $15.00 USD Received 21 December 2005; revised 30 January 2006; accepted 31 January 2006

challenging as the technique involves etch and re-growth steps to invert the domain of the nonlinearity in the semiconductor and hence adding AlGaAs is at best challenging. Operational table-top OPOs were demonstrated using these materials nonetheless [7]. From the aforementioned overview it is clear that a means of phase matching, which has low insertion loss, large nonlinear coefficient, and can be readily integrable with mainstream photonic devices using the available technologies is yet to be found.

In this work we present a simple means to achieve phase matching in compound semiconductor heterostructures through the use of novel waveguide design [8]. In this work phase matching is theoretically demonstrated through second harmonic generation (SHG) using a TE-polarized pump at 1550 nm wavelength which produces a TM-polarized SH radiation at 775 nm. Parametric conversion can also be demonstrated using the same structure by launching a TM-polarized SH at 775 nm; TE-polarized parametric florescence can then be obtained at 1550 nm.

The paper is organized as follows; in Section 2 the properties of Bragg reflection waveguides (BRWs) will first be discussed, then a demonstration of how these waveguides provide a propagation constant lower than that of the constituent waveguide materials will be presented. In Section 3, the mathematical formulation that describes the wave propagation in BRWs will be given, then in Section 4 the waveguiding condition for a BRW will be solved simultaneously with that describing waveguiding in conventional total internal reflection (TIR) waveguides, to obtain a structure that satisfies the condition $n_{2\omega} = n_{\omega}$. A discussion of this technique will be presented in Section 5 followed by a study of the tuning behavior in Section 6.

2. Features of Bragg reflection waveguides

The BRWs operates by providing reflection for one of the guided waves involved in the SHG process described above using stacks of periodic or quasi periodic layers on both sides of the core, as can be seen in Fig. 1. These waveguides have attracted substantial interest since their initial analysis [9]. Their interesting birefringence properties [10,11] were utilized to produce devices such as polarization splitters/combiners [12] while their versatile waveguiding properties were used to tailor the profile of their guided modes [13]. BRWs are also attractive for nonlinear propagation, where spatial optical solitons have been studied [14], and nonlinear optical modes have been found to propagate at higher optical powers in waveguides that have no bound modes in the linear regime [15].

One attractive feature in BRWs is their ability to provide lossless bound modes with modal effective indices that are much lower than the material indices of the waveguide material constituents, [9] when compared to the effective indices obtained for conventional TIR modes. This feature is utilized in our work to provide phase matching for a SHG process. This feature can be appreciated when the TIR and BRW mode indices of the same structure are

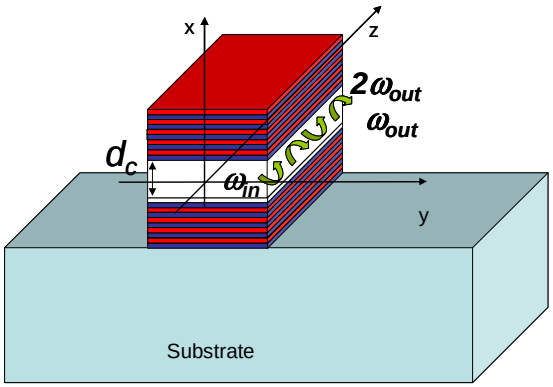

Fig. 1. A schematic diagram of a BRW with the propagation direction orthogonal to the Bragg stack.

#10071 - $15.00 USD Received 21 December 2005; revised 30 January 2006; accepted 31 January 2006

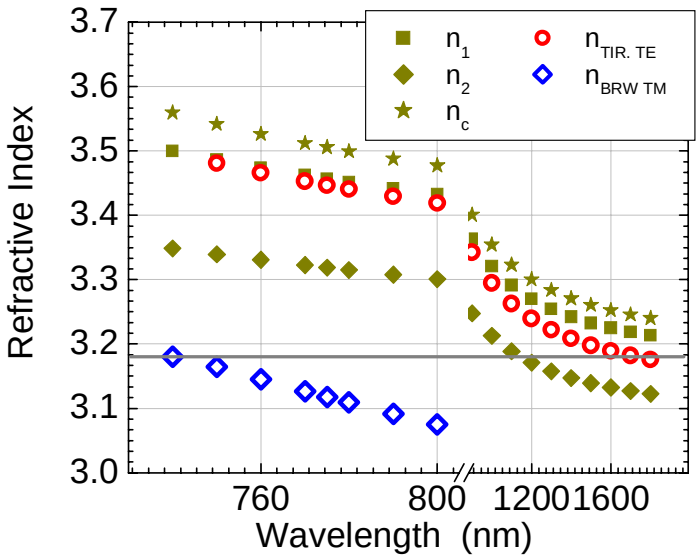

Fig. 2. Plot of the refractive index dispersion of a BRW similar to that shown in Fig. 1. The waveguide structure that resulted in this dispersion curve is a 200 nm core (n_c) of $Al_{0.24}G_{0.76}aAs$, sandwiched in a Bragg stack made of alternating layers of $Al_{0.3}G_{0.7}aAs$ and $Al_{0.5}G_{0.5}aAs$ (n_1 and n_2).

investigated on the same graph along with the material refractive indices of the structure. In Fig. 2 we chose a structure with core refractive index higher than both claddings, in order to provide conventional TIR. The waveguide structure that results in this dispersion curve is a 200 nm core of $Al_{0.24}G_{0.76}aAs$, sandwiched in a Bragg stack made of alternating layers of $Al_{0.3}G_{0.7}aAs$ and $Al_{0.5}G_{0.5}aAs$. As can be expected, the zero-order TIR modal index is lower than that of the core index by a factor of 2 %. In contrast, when the BRW mode of the same waveguide is examined, it is easy to observe that at any given wavelength, its effective index is lower than the core index and those of the cladding by at least 12 %. This property can then result in the BRW mode index, at a wavelength close to the core material bandgap, being equal to that of the zero-order TIR mode, at a wavelength further away than the material bandgap, as can be seen in Fig. 2. This property of BRWs has been observed previously and is documented but has not been used for the purpose of phase matching, to the best of our knowledge. Such waveguides can hence be used to provide guiding for the SH wavelength. It is worth noting that we have studied the material dispersion in this optical system experimentally using recent grating assisted measurements which lead to improved resolution to the existing measurements, and hence we have a reasonable handle on the refractive index values within this operating regime [16]. In the next section we shall present the waveguiding condition for BR waveguides.

3. Waveguiding condition for Bragg reflection waveguides

Assuming invariance in the *y* direction, the electric field propagating in the waveguide seen in Fig. 1 can be written as,

#10071 - $15.00 USD Received 21 December 2005; revised 30 January 2006; accepted 31 January 2006

$$E(x,z,t)=\begin{cases} E_K(x-d_c/2)e^{-iK(x-d_c/2)}e^{i(\omega t-\beta z)} & \mathrm{x}>\dfrac{d_c}{2} \\ \left[C_1\cos(k_c x)+C_2\sin(k_c x)\right]e^{i(\omega t-\beta z)} & -\dfrac{d_c}{2}<\mathrm{x}\le\dfrac{d_c}{2} \\ E_K(x+d_c/2)e^{iK(x+d_c/2)}e^{i(\omega t-\beta z)} & \mathrm{x}\le-\dfrac{d_c}{2} \end{cases} \quad (1)$$

where β is the wave vector in the direction of propagation, K is the Bloch wave vector in the periodic claddings, k_c is the wave vector in the core guiding layer, d_c is the core thickness and ω is the angular frequency of the wave at the operating wavelength. $E_K(x)$ is periodic with period Λ, where Λ is the period of the cladding and is equal to $\Lambda=d_1+d_2$, while d_1 and d_2 are the widths of both layers in the cladding stacks. The constants C_1 and C_2 are zero for odd and even modes respectively. The propagation coefficients are related such that,

$$k_c^2=\left(\frac{\omega.n_c}{c}\right)^2=\beta^2+k_x^2 \quad (2)$$

Where k_x is the wave vector in the waveguide transverse direction.

For second order nonlinear optics applications the overlap between the intensity of the fundamental and the field of the SH determines the efficiency of the interaction. Therefore this overlap needs to be a controllable parameter which can be optimized in order to provide efficient interactions. One simple means to maximize the overlap is to maximize the overlap of both modes in the core layer, which will be discussed in more detail in the forthcoming section. To achieve this goal using the minimum number of cladding layers, we shall use quarter-wavelength stacks [9,10]. Quarter-wavelength stacks help simplify the analysis as it keeps the formulae in a closed analytical form. These solutions also provide the highest confinement within the core by providing the largest exponential decay coefficient for the modal profiles within the claddings. This property dictates that,

$$k_{ix}d_i=\frac{\pi}{2}, \qquad i=1,2 \quad (3)$$

$$k_{ix}^2=\left(\frac{\omega.n_i}{c}\right)^2-\beta^2, \qquad i=1,2 \quad (4)$$

where k_{1x}, k_{2x} are the transverse wave vectors in both stack layers. In the special case of quarter-wavelength stack, the waveguiding condition then becomes [9,10],

$$\begin{aligned} ik_{1x}\frac{e^{iK\Lambda}+k_{1x}/k_{2x}}{e^{iK\Lambda}+k_{2x}/k_{1x}} &= \begin{cases} -k_c\tan(k_c d_c) & \text{for even TE modes} \\ k_c\cot(k_c d_c) & \text{for odd TE modes} \end{cases} \\ i\frac{k_{1x}}{n_c^2}\frac{e^{iK\Lambda}+n_2^2k_{1x}/n_1^2k_{2x}}{e^{iK\Lambda}+n_1^2k_{2x}/n_2^2k_{1x}} &= \begin{cases} -k_c/n_1^2\tan(k_c d_c) & \text{for even TM modes} \\ k_c/n_1^2\cot(k_c d_c) & \text{for odd TM modes} \end{cases} \end{aligned} \quad (5)$$

This condition is obtained through matching the field and its derivative ($\partial/\partial x$) at the interfaces of the core with both claddings to satisfy the necessary guiding condition for a bound mode. By designing the structure using quarter-wavelength stacks in the claddings we ensure that we operate right at the center of the stop band of the Bragg stack. This Bloch wave vector K is in the form,

$$K=\frac{m\pi}{\Lambda}\pm i\kappa_i, \qquad m=1,2.. \quad (6)$$

#10071 - $15.00 USD Received 21 December 2005; revised 30 January 2006; accepted 31 January 2006

The imaginary component κ_i determines the exponential decay/growth of the BR mode envelope into the claddings, and will be at a maximum in the center of the forbidden gap with a sign appropriate for field decay, which is described as follows for the quarter-wavelength claddings [17],

$$\Lambda\kappa_i \approx \begin{cases} \ln\left(\dfrac{k_{2x}}{k_{1x}}\right) & \text{for TE modes} \\ \ln\left(\dfrac{n_1^2 k_{2x}}{n_2^2 k_{1x}}\right) & \text{for TM modes} \end{cases} \tag{7}$$

From this equation it can be seen that the ratio of the stack refractive indices can be utilized to maximise the intensity of the BR mode in the core. The versatility in the design of propagation constant β, group velocity dispersion, and mode shapes afforded by BRWs is substantial. The mode shapes of these waveguides have also been studied recently [13]. In this work we shall restrict the discussion to the analysis of the quarter-wavelength cladding stacks as it is ideally suited for the design problem studied and as they also simplify the analysis of the structure, by avoiding numerical techniques for solution. In the analysis presented here the BRW modal index is assumed to provide real wave vectors for the mode throughout all the layers. Other operating regimes where this condition does not apply are also of interest but will be analyzed elsewhere.

A question may arise about how we define the thicknesses of the cladding layers d_1 and d_2 prior to the design. In our case of quarter-wavelength claddings both thicknesses are defined as per Eq. (3), and hence can be expressed as a function of the propagation constant and the wave vector of their respective layer. This enables their determination after solving for the propagation constantβ. Therefore there is no need for prior knowledge of d_1 and d_2 when using the method described here since we inherently set their contribution ($k_i d_i$) to be $\pi/2$. In the section that follows we shall simultaneously solve the waveguiding condition of both the TIR and BRW modes for a given waveguides in order to fulfill the condition $n_{2\omega} = n_{\omega}$.

4. Simultaneously solving for TIR and BRW waveguiding conditions

The BRW is used to compensate for the large difference in the propagation constant of the fundamental and SH waves (@ 775 nm) due to material dispersion by providing a guided mode at the SH. Henceforth a TIR waveguide for the fundamental wave (@ 1550 nm) needs to be designed in the structure. For this purpose we use a core of higher refractive index to provide TIR waveguiding @ 1550 nm. Owing to the one dimensional nature of the problem at hand and the stratified periodic medium, the fundamental mode can therefore be easily analysed using the field transfer matrix method [18]. The technique is very well documented else where and is based on constructing a transfer matrix for the layer stack, which accounts for the phase accumulated in every layer [18],

$$M_{structure} = \begin{pmatrix} m_{11} & m_{12} \\ m_{21} & m_{22} \end{pmatrix} = \prod_{j=1}^{l} M_j, \quad \text{total number of layers} = l \tag{8}$$

The initial layer matrices M_j are defined as,

$$M_j = \begin{pmatrix} \cos\Phi_j & \dfrac{-i}{\gamma_j}\sin\Phi_j \\ -i\gamma_j \sin\Phi_j & \cos\Phi_j \end{pmatrix} \tag{9}$$

$$\Phi_j = k_{jx} d_j \tag{10}$$

#10071 - $15.00 USD Received 21 December 2005; revised 30 January 2006; accepted 31 January 2006

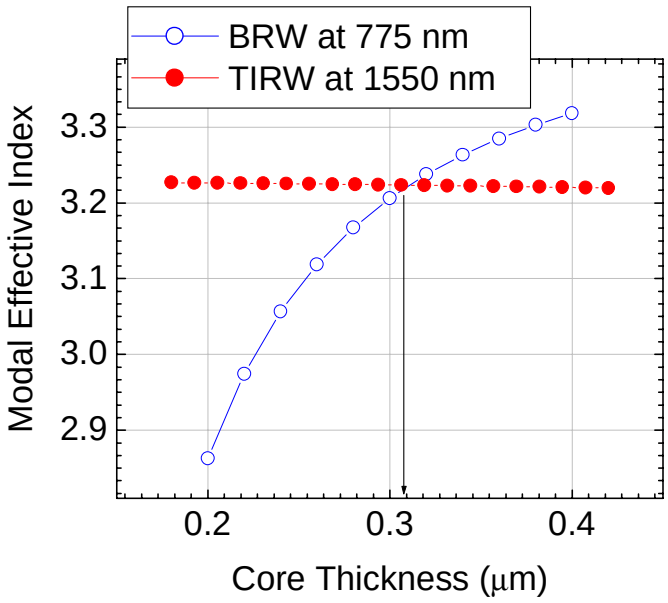

Fig. 3. A graphical example of the solution of both the TIR and BR modes. The waveguide structure that resulted in this dispersion curve is a 310 nm core of 30% AlGaAs, sandwiched in a Bragg stack made of alternating quarter wave layers of 20% and 40% AlGaAs.

$$\gamma_j = \begin{cases} \dfrac{\sqrt{n_j^2 - n_{eff}^2}}{c\mu_o} & \text{for TE modes} \\ \dfrac{\sqrt{n_j^2 - n_{eff}^2}}{c\varepsilon_o} & \text{for TM modes} \end{cases} \tag{11}$$

where c, μ_o, ε_o, n_{eff}, d_j, n_j, k_{jx} are the speed of light, vacuum permeability, vacuum permittivity, effective modal index, thickness, refractive index and propagation constant in x direction of layer j respectively. The modal dispersion function can be written as,

$$\chi_M(n_{eff}) = \gamma_c m_{11} + \gamma_c \gamma_s m_{12} + m_{21} + \gamma_s m_{22}, \tag{12}$$

where γ_c and γ_s are the γ parameter for the top cladding and substrate of the layers respectively. For lossless bound modes the modal dispersion function is imaginary [18]. Therefore to obtain the zero-order fundamental mode at 1550 nm $\chi_M(n_{eff}) = 0$ is solved for the structure studied. However in order to preserve self consistency, $\chi_M(n_{eff})$ needs to be solved simultaneously with Eq. (5) to obtain the SH and fundamental modes with an identical propagation constant. For demonstration, the solutions from both Eq. are plotted graphically and the intersection point represents the solution as shown in Fig. 3 for the device parameters discussed below.

The core is made of $Al_{0.3}G_{0.7}aAs$ layer, while the quarter-wavelength Bragg stacks on either side are made of alternating $Al_{0.2}G_{0.8}aAs$ and $Al_{0.4}G_{0.6}aAs$. For demonstration purposes both Eqs. (5) and (13) are solved and presented here graphically. As can be seen in Fig. 3, the propagation constant of both modes match at a core thickness of 310 nm. The respective

#10071 - $15.00 USD Received 21 December 2005; revised 30 January 2006; accepted 31 January 2006

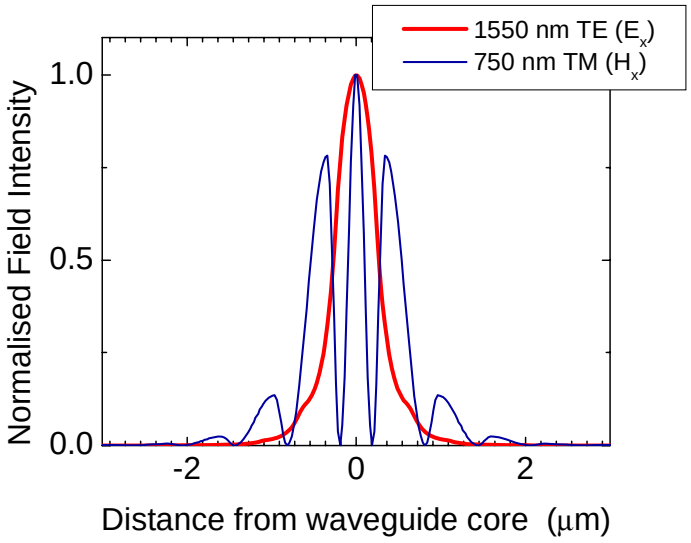

Fig. 4. Field profiles of both the TE-polarized TIR mode @ 1550 nm and the TM-polarized BRW mode at 775nm.

modes are then calculated and plotted, as shown in Fig. 4, where the 45% of the TE mode of the fundamental at 1550 nm is spatially centered in the core of the structure overlapping with 23 % of the SH field which is the TM BR mode at 775 nm. The effective index of these guides coincided at a value of 3.2236 for this structure.

5. Discussion

As can be seen from the field profiles in Fig. 4, the spatial mode overlap of the interacted intensities is considerable, which is not always the case for some of the other phase matching techniques. However the conversion efficiency between the modes depends on the spatial overlap between the induced dielectric polarization at 2ω, $P^{2\omega}(x) = \varepsilon_0 d(x)[E^{\omega}(x)]^2$, and the field of SH mode, $E^{2\omega}(x)$, where $d(x)$ is the effective nonlinear coefficient [19]. This implies that the conversion efficiency is reduced due to the regions within the cladding where $E^{2\omega}(x)$ goes out of phase from $[E^{\omega}(x)]^2$. One intuitive route to maximize the fields' overlap is to maximize the core confinement. In this case the confinement is ~ 45 % and that of the SH is ~ 23 %, which is considerable for an initial design without exhaustive optimization. However it is imperative to take into account that the case presented here is generic, without a thorough optimization procedure for mere proof of principle. BRWs provide extensive degrees of design freedom to control the field decay in the cladding, modal shapes, overlap and dispersion. Hence they hold tremendous potential for maximizing the overlap and hence the conversion efficiency. For the case studied here the conversion efficiency is comparable to those of modal phase matching [19].

The design presented here is in principle a mode matching technique. However it differs from previously reported methods [20,21] in that the modal properties of both modes offer an extra degree of freedom for optimisation. The BRW and TIR modes used here can be optimized more independently using the degrees of freedom afforded by the quarter-wavelength BRWs. For example, the quarter-wavelength stacks used here can be of any AlGaAs composition provided that the $\pi/2$ phase shift condition in Eq. (3) is fulfilled, which allows tailoring the confinement of the TIR mode with minimal influence on the BRW mode properties. Some limitations will still apply nonetheless, as the propagation constant cannot be

#10071 - $15.00 USD Received 21 December 2005; revised 30 January 2006; accepted 31 January 2006

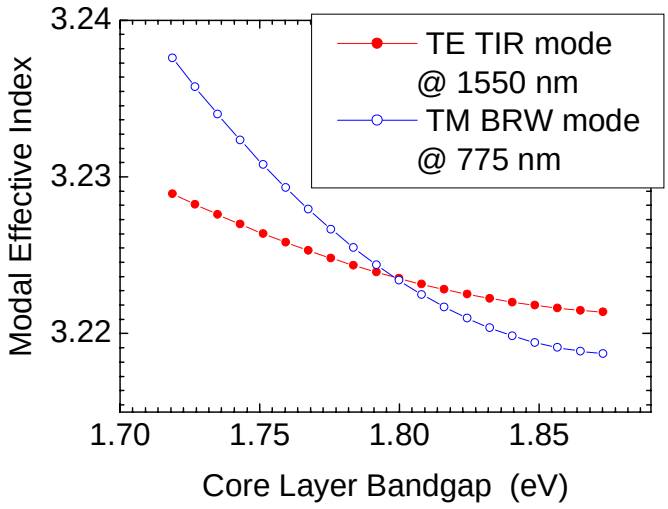

Fig. 5. Modal index of both the TIR and BR modes due to the change of the core bandgap, and hence refractive index.

increased indefinitely for example, to avoid evanescent fields in the cladding, and the resulting excessive losses. Some of the reported techniques involve coupling between the fundamental and higher order modes, which limit the spatial overlap and hence the conversion efficiency of these techniques [20]. The challenge there is to maximize the overlap integral between the interacting waves. Another technique relies on coupled waveguides [21]. Such coupled waveguides were reported to have potential conversion efficiency of 100%. Practical implementation may suffer from excess losses due to the fabrication tolerances of the coupler. In contrast the technique presented here is implemented in a single waveguide defined by Bragg stacks which has been studied extensively and shown to have extremely low loss from work on vertical cavity surface emitting lasers [22]. In addition the waveguides presented here offer ample room for optimizing the overlap integral between the interacting waves. A comparison with PPLN is not possible simply because PPLN is inherently less efficient by virtue of being a quasi-phase matching technique, in contrast to the exact phase matching proposed here. In addition, the nonlinear coefficient for GaAs is ≈1 order of magnitude larger than the effective coefficient of PPLN. Gain through carrier injection, fast precise carrier tuning and fabrication technologies are all factors that render a semiconductor-based nonlinear device to be favourable, even if the efficiency is comparable to that of PPLN.

The technique discussed here uses type-I phase matching which couples a TE-polarized pump at the fundamental wavelength with a TM-polarized wave at the SH. This type has been demonstrated using other modal phase matching techniques before [3] as well as quasi phase matching techniques [4]. Another possible configuration for our structure is type-II phase matching which couples a mixed TE-TM-polarized wave at the fundamental with a TE-polarized SH. Again this type follows identical principles to what we have discussed in this work. It has been demonstrated using a different modal phase matching technique recently [20]. As such, if there is any other mode within the structure we study here to which there can be power transfer from the fundamental, it needs to be TM-polarized due to the type-I phase matching used. The waveguide was designed such that the only guided TIR mode at the SH is the zero-order TE-polarized mode, hence no coupling is likely to occur. Moreover, BRWs have also been known to support interface modes. These modes are however loosely bound, and more importantly they concentrate the energy around the interfaces of the core with the Bragg stacks. This leads to an overlap integral which is substantially lower than that available between the zero-order TIR mode at 1550 nm and the zero-order BRW mode at 775 nm.

#10071 - $15.00 USD Received 21 December 2005; revised 30 January 2006; accepted 31 January 2006

Therefore the effect of such modes, if they exist, on the efficiency of second harmonic generation is thought to be negligible.

6. Tuning

Tuning is essential for the majority of the applications for SHG. This device can be tuned using electro-optic or carrier induced effects in a *p-i-n* doped structure where the intrinsic layer overlaps chiefly with the core. Hence the refractive index of the core waveguide can be tuned using current or potential [8]. This will accordingly change the modal effective indices at both the fundamental and SH. The effect is shown in Fig. 5 where the modal indices overlap as the starting material bandgap, which in our case being $Al_{0.3}G_{0.7}As$. In this plot it is assumed that the refractive index change is caused by a change in the bandgap; however the effect is the same if current or other effects are used for tuning. One of the attractive features of using BRWs is that the waveguide dispersion can be tailored to minimise the mismatch with that of the TIR mode at the fundamental; however this entails using BR stacks that are much more complex than the quarter-wavelength plate used here, and hence will be presented elsewhere. Although thermal tuning is also possible, it is of less practical use in compound semiconductors, as more effective means are available for tuning, including electro optic and carrier tuning.

The bandwidth of the BR mode depends on that of the bandgap of the cladding Bragg stack, which for a quarter-wavelength structure has a bandwidth [17],

$$\Delta\omega_{gap} \approx \omega_o \frac{2}{\pi}\left(\frac{k_{2x} - k_{1x}}{k_{2x}}\right), \tag{13}$$

However the actual bandwidth of the phase matching waveguide is likely to be limited by the overall dispersion, with the material and modal dispersion at the SH being the dominant factor. This can be seen from the material dispersion as shown in Fig. 2, the waveguide dispersion depicted in Fig. 5.

The design offers distinct advantages over the techniques which have been developed previously;

- No patterning along the direction of propagation and hence have the potential to possess low optical losses in comparison with other quasi-phase matching designs. However it must be noted that Fresnel and modal phase matching share this advantage with our technique.
- Gain can be provided in structures through carrier injection via electrical pumping. The electrical pumping is readily available in such structures due to the work which has been carried out developing vertical cavity surface emitting lasers.
- The structure lends itself to be grown along side active and passive photonic devices for monolithic integration.

7. Conclusions

A design which utilizes Bragg reflector waveguides to provide phase matching for second harmonic generation at a wavelength of 775 nm is reported for the first time. The structure offers an attractive alternative to the techniques investigated to date as it involves no patterning along the propagation direction and allows more control over the overlap between the interacting waves and hence lends itself to more efficient nonlinear interactions. However the bandwidth efficiency and tuning capabilities of this phase matching technique need to be experimentally verified.

Acknowledgments

The Author would like to thank I. Golub and Brian R. West for stimulating discussion. This work has been supported by the department of ECE at the University of Toronto and NSERC.

#10071 - $15.00 USD Received 21 December 2005; revised 30 January 2006; accepted 31 January 2006